

# Segmentation as Postprocessing for Hyperspectral Image Classification

Luis Ignacio Jiménez  
and  
Antonio Plaza  
Hyperspectral Computing Laboratory,  
Department of  
Technology of Computers  
and Communications,  
University of Extremadura, Caceres, Spain  
[www.unex.es/investigacion/grupos/hypercomp](http://www.unex.es/investigacion/grupos/hypercomp)

Victor Andrés Ayma,  
Pedro Achanccaray  
and  
Gilson A.O.P. Costa  
Computer Vision Lab,  
Catholic University  
of Rio de Janeiro,  
Rio de Janeiro, Brasil  
[www.lvc.ele.puc-rio.br/wp/](http://www.lvc.ele.puc-rio.br/wp/)

Raul Queiroz  
Feitosa  
Computer Vision Lab,  
Catholic University  
of Rio de Janeiro  
and  
Department of Computer Engineering,  
Rio de Janeiro State University,  
Rio de Janeiro, Brasil  
[www.lvc.ele.puc-rio.br/wp/](http://www.lvc.ele.puc-rio.br/wp/)

**Abstract**—Hyperspectral imaging is a technique in remote sensing that collect hundreds of images at different wavelength values in the same area of the Earth. For instance, the Airborne Visible Infra-Red Imaging Spectrometer (AVIRIS) sensor of NASA capable to obtain 224 spectral channels in a wavelength range between 400 and 2500 nanometers. As a result, each pixel of the image can be represented as a spectral signature. Image segmentation is the process of dividing a digital image into groups of pixels or objects. Hyperspectral image classification is an important and active area dedicated to identifying each pixel in the image with an exclusive material/object class. Several efforts had been done in this field using spectral and spatial information separately or simultaneously due to improve the performance of the classification techniques. In previous works have been used similar techniques using spectral and spatial information separately or simultaneously. In this work we have focused on a region-growing segmentation algorithm, applied as postprocessing on the standard classification, produces by a SVM classifier, in order to improve the performance of the classification technique. Experimental results with a real hyperspectral data set over the city of Pavia are included.

## I. INTRODUCTION

Hyperspectral image classification has been a very active area of research in recent years [1]. Given a set of observations (*i.e.*, pixel vectors in a hyperspectral image), the goal of classification is to assign a unique label to each pixel vector so that it is well-defined by a given class. Several efforts have been performed in the literature in order to integrate spatial-contextual information in spectral-based classifiers for hyperspectral data [2]. It is now commonly accepted that using the spatial and the spectral information simultaneously provides significant advantages in terms of improving the performance of classification techniques [3]. Some of these approaches include spatial information prior to the classification, during the feature extraction stage [4]. Another strategy in the literature has been to exploit simultaneously the spatial and the spectral information [5]. Several other approaches include spatial information as a post-processing, *i.e.*, after a

spectral-based classification has been conducted. One of the first classifiers with spatial post-processing developed in the hyperspectral imaging literature was the well-known ECHO (extraction and classification of homogeneous objects) [1]. Another one is the strategy adopted in [6], which combines the output of a pixel-wise support vector machine (SVM) classifier with the morphological watershed transformation [7] in order to provide a more spatially homogeneous classification. A similar strategy is adopted in [8], in which the output of the SVM classifier is combined with the output provided by the recursive hierarchical segmentation (RHSEG) segmentation algorithm.

In this work, we develop a new technique that uses segmentation as a post-processing for standard (pixel-wise) hyperspectral image classification. Specifically, we use a multiresolution algorithm proposed by Baatz and Schäpe [9] which is considered one of the most effective segmentation algorithms in the literature. Here, we have considered a version based on the local mutual best fitting heuristic [10], which generates the segmentation using region growing techniques. In the following, we describe the methodology adopted for segmentation as a post-processing of hyperspectral image classification (conducted in this work using the standard SVM classifier). The paper concludes with an experimental evaluation of the newly proposed approach using the well-known hyperspectral image collected by the Reflective Optics Spectrographic Imaging System (ROSIS) over the University of Pavia, Italy.

## II. MULTIREOLUTION ALGORITHM

As is shown in Alg.1 the segmentation algorithm is divided in different stages: 1) initialization of seeds, considering each pixel of the image as a segment and seed at the same time; 2) evaluation of the spatial neighborhood and identification of the best neighbor for each segment; 3) test the mutual best fitting heuristic; 4) fusion, where all segment markers whose merging cost is lower than the square of a scale parameter are merged.

---

**Algorithm 1** Pseudocode of Region Growing Multiresolution Algorithm

---

```

image = ReadImage
img = SeedInitialization()
while has merge
    FindBestNeighbor()
    if found
        if TestMutualBestNeighbor()
            Fusion()
            RemoveSegmentFromList()
            UpdateSegment()
        end if
    end while

```

---

The growth of the segments is constrained, therefore, an adjustable criteria of heterogeneity. This adjustment can be done by choosing the *scale* parameter, the weights of the spectral bands ( $w_c$ ), the factor of *color* and the *compactness* factor. The changes on the scale parameter directly influence the size of the generated segments. Moreover, the relevance of each spectral band, in our case same weight for each band, the relative importance of shape and color, and between compactness and smoothness, can be adjusted through the parameters of the algorithm as is shown in 1.

$$f = w_{color} * h_{color} + (1 - w_{color}) * h_{shape} \quad (1)$$

Equation 2 shows the formulation of spectral heterogeneity ( $h_{color}$ ); where the selected segment is  $obj_1$ ,  $obj_2$  is the analyzed neighbour and the  $obj_3$  is the result of merge with  $obj_1$  and  $obj_2$ . The index of the spectral band is named as  $c$  and  $w_c$  is the weight set for band  $c$  (in our case, the same for each one of them);  $\sigma$  is the standard deviation of the pixels in the band  $c$ , considering all the pixels belonging to segment  $obj_i$ ; and  $n$  is the number of pixels in  $obj_i$ , for  $i = 1, 2, 3$ .

$$h_{color} = \sum w_c (n_{obj_3} * \sigma^{obj_3} (n_{obj_1} * \sigma^{obj_1} - n_{obj_2} * \sigma^{obj_2})) \quad (2)$$

In Equation 3 is defined the spatial heterogeneity, which at the same time, is calculated based on the compactness  $h_{cmpct}$ , shown in Equation 4, and the smoothness  $h_{smooth}$ , described in Equation 5, components. Both of these componest are measure by the factor of compression  $w_{cmpct}$  intoudced as parameter.

$$h_{shape} = w_{cmpct} * h_{cmpct} + (1 - w_{cmpct}) * h_{smooth} \quad (3)$$

$$h_{cmpct} = n_{obj_3} * \frac{l_{obj_3}}{\sqrt{n_{obj_3}}} - (n_{obj_1} * \frac{l_{obj_1}}{\sqrt{n_{obj_1}}} + n_{obj_2} * \frac{l_{obj_2}}{\sqrt{n_{obj_2}}}) \quad (4)$$

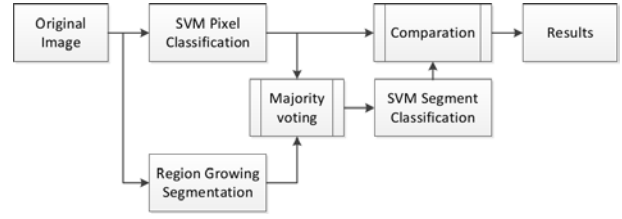


Fig. 1. Flowchart of the proposed technique for segmentation as postprocessing to hyperspectral classification.

$$h_{smooth} = n_{obj_3} * \frac{l_{obj_3}}{\sqrt{b_{obj_3}}} - (n_{obj_1} * \frac{l_{obj_1}}{\sqrt{b_{obj_1}}} + n_{obj_2} * \frac{l_{obj_2}}{\sqrt{b_{obj_2}}}) \quad (5)$$

In these equations  $l$  is the perimeter of the segment  $obj_i$  and  $b$  the perimeter of the corresponding minimum bounding box, for  $i = 1, 2, 3$ .

Once a first segmentation has been obtained, the algorithm performs a step in which the segments are redefined by setting the rest of the pixels of the merged segments as belonging to the resulting segment. Finally, the segmentation process concludes by a step in which the borders are recalculated by updating the pixel-segment structures. These steps are repeated until there are no more segments that can be merged.

### III. METHODOLOGY

Fig. 1 shows a flowchart of the methodology used in this work. First, the original hyperspectral image is classified in pixel-wise fashion using the SVM classifier and at the same time, the segmentation step is conducted. At this point both the pixel-wise classification and the segmentation of the original hyperspectral image have been completed. Now, as shown in Fig. 1, we perform a fusion of the results obtained by the classification and the segmentation using majority voting. This procedure is inspired by the one conducted in previous works [8], and consists of using the regions obtained in the segmentation as superpixels with a unique class represented in them. The decision on which class should be assigned to each superpixel is taken based on the total number of pixels belonging to the superpixel that are assigned to each given class in the pixel-wise classification. In other words, if a superpixel has a majority of pixels assigned to a given class in the pixel-wise classification, all the superpixel (region) is assigned to that given class. The output of this step is identified as SVM segment classifier in Fig. 1 Finally, we perform a comparison of the classification results obtained using this procedure with regards to the ground-truth.

### IV. EXPERIMENTAL RESULTS

Our experiments were conducted using a popular hyperspectral image collected over the University of Pavia, Italy, by the ROSIS instrument. The image size in pixels is  $610 \times 340$ , with spatial resolution of 1.3 meters per pixel and 103 spectral bands in the range from 0.41 to 0.82 micrometers. The ground-truth comprises nine mutually exclusive classes, displayed in Fig.2.

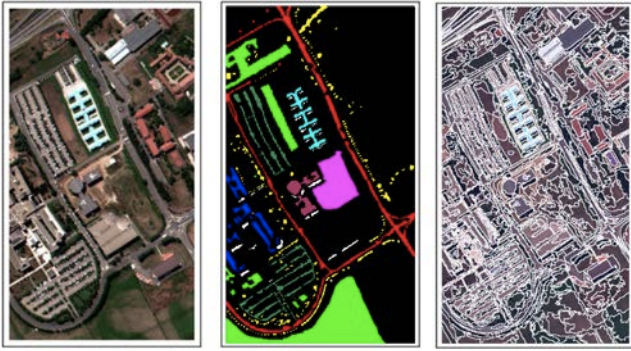


Fig. 2. ROSIS Pavia University scene. Left: true color composition. Middle: ground-truth map containing nine mutually exclusive classes. Right: Segmented Image

The configuration of the segmentation algorithm used in experiments was conducted as follows. The *scale* parameter, which directly influences the size of the regions or superpixels, was empirically set to  $scale = 58$  (the minimum value of this parameter is 0, and the maximum value is 100). The relative weight between color and shape, another required parameter for the segmentation algorithm, was set to  $color = 0.2$ . Finally, a *shape* parameter which is related to spatial heterogeneity was set to  $shape = 0.9$ . For the latter two parameters, the minimum value is 0 and the maximum value is 1. We emphasize that these parameter settings were optimized, based on the classification results obtained at the end of the methodology chain, after many tests. The SVM classification was conducted using the Gaussian Radial Basis Function (RBF) kernel, and the optimal parameters  $C$  and  $\gamma$  were determined using the values set as reference in previous works [11]:  $C = 128$ ,  $\gamma = 0.125$ . Table 1 reports the overall accuracy (OA) and the individual class accuracies obtained using the pixel-wise SVM classification and the proposed method, which refines the SVM classification using the considered segmentation algorithm. Table 1 reveals significant increase of the OA and the individual class accuracies, which is related to the consideration of spatial information (in the form of superpixels) by including the proposed segmentation-based postprocessing approach. For illustrative purposes, Fig. 3 shows some of the classification results obtained after applying the SVM pixel-wise classification (middle), the segmentation-refined classification (right) obtained after combining the segmentation and classification results by means of majority voting and the reference data used to measure the results. As shown by the rightmost classification map in Fig. 3, the proposed approach provides better results in segments widely represented by one class and those segments that represents major objects, like buildings. In general, provides a smoother classification output with spatial consistency and sharp edges.

## V. CONCLUSIONS AND FUTURE RESEARCH

In this work we have presented a new technique for hyperspectral image classification which uses the segmentation algorithm proposed by Baatz and Schäpe as a postprocessing

for a standard pixel-wise classification using support vector machines. The segmentation is conducted by means of a region growing multiresolution technique that generates a set of superpixels which are then classified using majority voting by considering the predominant classification label on the associated pixels. The proposed approach is simple, but leads to a significant improvement in the obtained classification results. This suggests the potential of combining segmentation and classification techniques for enhancing the interpretation of hyperspectral image data. The main drawback of the proposed method, which is yet to be resolved in future developments, is the cost of the optimization of the multiresolution algorithm. Our future work will be focused on automating this procedure and reducing the cost by exploring high performance computing implementations in parallel computing architectures.

## ACKNOWLEDGMENT

The authors would like to gratefully thank the funding from the Marie Curie Action for International Research Staff Exchange Tools for Open Multi-Risk Assessment Using Earth Observation Data (TOLOMEO) provided by the European Commission.

## REFERENCES

- [1] D. A. Landgrebe, *Signal Theory Methods in Multispectral Remote Sensing*, John Wiley & Sons: New York, 2003.
- [2] A. Plaza, J. A. Benediktsson, J. Boardman, J. Brazile, L. Bruzzone, G. Camps-Valls, J. Chanussot, M. Fauvel, P. Gamba, J.A. Gualtieri, M. Marconcini, J. C. Tilton, and G. Trianni, "Recent advances in techniques for hyperspectral image processing," *Remote Sens. Environment*, vol. 113, pp. 110–122, 2009.
- [3] M. Fauvel, Y. Tarabalka, J.A. Benediktsson, J. Chanussot, and J.C. Tilton, "Advances in spectral-spatial classification of hyperspectral images," *Proceedings of the IEEE*, vol. 101, no. 3, pp. 652–675, March 2013.
- [4] J.A. Benediktsson, J.A. Palmason, and J.R. Sveinsson, "Classification of hyperspectral data from urban areas based on extended morphological profiles," *IEEE Trans. Geosci. and Remote Sens.*, vol. 43, no. 3, pp. 480 – 491, 2005.
- [5] J. Li, P. Marpu, A. Plaza, J. Bioucas-Dias, and J. A. Benediktsson, "Generalized composite kernel framework for hyperspectral image classification," *IEEE Trans. Geosci. and Remote Sens.*, 2013, in press.
- [6] Y. Tarabalka, J. Chanussot, and J.A. Benediktsson, "Segmentation and classification of hyperspectral images using watershed transformation," *Pattern Recogn.*, vol. 43, pp. 2367–2379, 2010.
- [7] P. Soille, *Morphological Image Analysis, Principles and Applications*, Berlin, Germany: Springer-Verlag, 2nd edition, 2003.
- [8] Y. Tarabalka, J. A. Benediktsson, J. Chanussot, and J. C. Tilton, "Multiple spectral-spatial classification approach for hyperspectral data," *IEEE Trans. Geosci. and Remote Sens.*, vol. 48, no. 11, pp. 4122–4132, 2011.
- [9] M. Baatz and A. Schäpe, "Multiresolution segmentation: an optimization approach for high quality multi-scale image segmentation," *Angewandte Geographische Informationsverarbeitung XII*, pp. 12–23, 2000.
- [10] P.N. Happ, R.Q. Feitosa, C. Bentes, and R.Q. Farias, "A parallel image segmentation algorithm on gpus," in *Proceedings of the International Conference on Geographic Object-Based Image Analysis (GEOBIA)*, 2012, vol. 4, pp. 580–585.
- [11] Yuliya Tarabalka, Jocelyn Chanussot, and Jon Atli Benediktsson, "Segmentation and classification of hyperspectral images using watershed transformation," *Pattern Recognition*, vol. 43, no. 7, pp. 2367–2379, 2010.

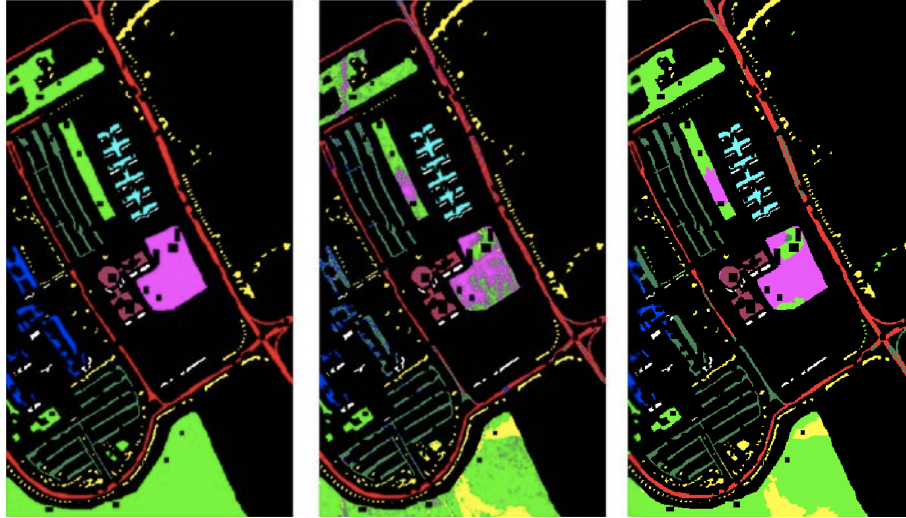


Fig. 3. Processing results. Left: Reference data classification. Middle: SVM Pixel-wise classification. Right: Result obtained after applying the proposed technique, which uses segmentation as a preprocessing for classification.

Class	SVM pixel-wise classification	Proposed approach
Asphalt	74.714	80.647
Meadows	77.620	85.022
Gravel	46.006	46.557
Trees	98.008	89.526
Metal Sheets	99.820	97.215
Bare Soil	66.185	83.377
Bitumen	83.690	97.554
Self-blocking Bricks	90.190	98.127
Shadow	100.000	99.623
Overall accuracy (OA)	78.174	84.766

TABLE I

OVERALL AND INDIVIDUAL ACCURACIES OBTAINED AFTER CLASSIFYING THE ROSIS PAVIA UNIVERSITY SCENE USING A STANDARD SVM PIXEL-WISE CLASSIFICATION AND THE PROPOSED APPROACH, WHICH INTEGRATES SEGMENTATION AND CLASSIFICATION.